PHYSICAL REVIEW A **74**, 063408 (2006)

Nuclear spin relaxation of ^{129}Xe due to persistent xenon dimers

B. N. Berry-Pusey, B. C. Anger, G. Laicher, and B. Saam

Department of Physics, University of Utah, Salt Lake City, Utah 84112-0830, USA

(Received 12 September 2006; published 15 December 2006)

We have measured longitudinal nuclear relaxation rates of ^{129}Xe in Xe-N_2 mixtures at densities below 0.5 amagats in a magnetic field of 8.0 T. We find that intrinsic spin relaxation in this regime is principally due to fluctuations in the intramolecular spin-rotation (SR) and chemical-shift-anisotropy (CSA) interactions, mediated by the formation of ^{129}Xe-Xe persistent dimers. Our results are consistent with previous work done in one case at much lower applied fields where the CSA interaction is negligible and in another case at much higher gas densities where transient xenon dimers mediate the interactions. We have verified that a large applied field suppresses the persistent-dimer mechanism, consistent with standard relaxation theory, allowing us to measure room-temperature gas-phase relaxation times T_1 for ^{129}Xe greater than 25 h at 8.0 T. These data also yield a maximum possible low-field T_1 for pure xenon gas at room temperature of 5.45 ± 0.2 h. The coupling strengths for the SR and CSA interactions that we extract are in fair agreement with estimates based both on previous experimental work and on *ab initio* calculations. Our results have potential implications for the production and storage of large quantities of hyperpolarized ^{129}Xe for use in various applications.

DOI: 10.1103/PhysRevA.74.063408 PACS number(s): 33.25.+k, 32.80.Bx, 34.30.+h

I. INTRODUCTION

The stable spin-$\frac{1}{2}$ isotopes ^{3}He and ^{129}Xe are readily polarized to levels exceeding 0.1 via spin-exchange optical pumping (SEOP) [1,2], making them accessible to a wide variety of magnetic resonance experiments. As the name "hyperpolarized" suggests, the relative populations of nuclear-spin sublevels in these gases are well out of thermal equilibrium; therefore an understanding of longitudinal relaxation mechanisms (characterized by the time T_1) that limit both the achievable polarization and the sample storage time is critically important. Several recently published papers [3–5], and references therein, discuss the physics and applications of hyperpolarized ^{3}He. We are concerned here specifically with hyperpolarized ^{129}Xe, which is also studied and used in a wide variety of applications, including recent examples in medical imaging [6], biochemistry [7], and surface science [8].

The gas-phase relaxation mechanisms may be divided broadly into intrinsic and extrinsic categories. The former are due to the presence of the other noble-gas atoms in the sample and include, for example, the dipole-dipole mechanism present during ^{3}He-^{3}He binary collisions that limits T_1 in a 1 amagat sample of ^{3}He to $\approx$800 h [9]. (One amagat $= 2.69 \times 10^{19}$ cm^{-3}, the density of 1 atm of an ideal gas at 0 °C. Unless otherwise noted, densities quoted here have been calculated from pressures measured at room temperature.) In practice, T_1 is usually limited by extrinsic mechanisms, including diffusion through external magnetic-field gradients [10,11] and (more often) collisions with container (cell) walls. However, more recent work, including that presented here, indicates that intrinsic mechanisms are far more important in many practical experiments involving ^{129}Xe than previously assumed. We thus generally describe the ^{129}Xe gas-phase relaxation rate Γ as the sum of four terms

$$\Gamma = \Gamma_t + \Gamma_p + \Gamma_g + \Gamma_w, \tag{1}$$

where the first two (intrinsic) terms are due, respectively, to transient and persistent xenon dimers (see below), and the last two (extrinsic) terms are due to gradient and wall relaxation, respectively.

A. Xenon dimers

Intrinsic gas-phase ^{129}Xe relaxation is related to the van der Waals forces that govern the formation of xenon dimers, and herein, we make an important distinction: *transient* dimers are formed in binary collisions, where the per-atom collision frequency $1/T_t$ is proportional to the xenon density [Xe] and the collision duration τ_t (a few picoseconds) depends on the details of the Xe-Xe interatomic potential; *persistent* dimers are formed by three-body collisions and exist in a stable bound state for a molecular lifetime τ_p until the next collision with another atom.

The possible existence of persistent dimers was suggested as early as 1959 by Bernardes and Primakoff [12], whose model can be used to estimated their concentration to be 0.5% for [Xe]=1 amagat. The dimer concentration is related to the chemical equilibrium coefficient $\mathcal{K} \equiv [Xe_2]/[Xe]^2$, from which we obtain the fraction of Xe atoms bound in Xe_2 molecules

$$\frac{2[Xe_2]}{[Xe]+2[Xe_2]} \approx 2\mathcal{K}[Xe], \tag{2}$$

where the approximation is very good in the limit where $[Xe_2] \ll [Xe]$. Chann *et al.* [13] calculated the partition function for the internal states of the Xe_2 molecule to arrive at $\mathcal{K} = 230$ Å^3, or a 1.2% persistent dimer concentration for [Xe]=1 amagat.

The calculated properties of the Xe-Xe interatomic potential and simple kinetic theory [14] allow reasonable estimates of the relevant kinetic parameters to be made. Here we assume thermal and chemical equilibrium and that Xe gas is the only constituent. The results are summarized in Table I. The velocity-averaged collision cross sections $\langle \sigma v \rangle_{Xe}$ and $\langle \sigma v \rangle_{Xe_2}$ are estimated as a product of relative rms speed and

TABLE I. Estimates of kinetic parameters [14] for transient and persistent xenon dimers in pure xenon gas in thermal and chemical equilibrium. The cross sections are calculated using the appropriate value of relative rms speed, $v_{\rm rms}=(8k_BT/\pi\mu)^{1/2}$, where k_B is the Boltzmann constant, T is temperature, and the reduced mass μ is 1/2 and 2/3 of the average (naturally abundant) Xe atomic mass for Xe-Xe and $XeXe_2$ collisions, respectively. The transient-dimer lifetime is calculated using $v_{\rm rms}=3.08\times10^4$ cm/s, appropriate for Xe-Xe binary collisions. The persistent-dimer lifetime is estimated under the assumption that all collisions break up the dimers and is about two orders of magnitude longer than the transient-dimer lifetime.

Quantity	Symbol	Formula	Value at 295 K, [Xe]=1 amagat
Xenon density	[Xe]		2.687×10^{19} cm^{-3}
Xe_2 equilibrium separation [15]	R_0		4.4 Å
Depth of Xe_2 potential well [15]	ϵ/k_B		283 K
Vel.-avged. Xe-Xe cross section	$\langle\sigma v\rangle_{\rm Xe}$	$\pi R_0^2 v_{\rm rms}$	1.9×10^{-10} cm^3/s
Vel.-avged. Xe-Xe_2 cross section	$\langle\sigma v\rangle_{\rm Xe2}$	$2\pi R_0^2 v_{\rm rms}$	3.25×10^{-10} cm^3/s
Time between transient collisions	T_t	$([{\rm Xe}]\langle\sigma v\rangle_{\rm Xe})^{-1}$	200 ps
Transient-dimer lifetime	τ_t	$2R_0/v_{\rm rms}$	2.85 ps
Persistent-dimer lifetime	τ_p	$([{\rm Xe}]\langle\sigma v\rangle_{\rm Xe2})^{-1}$	115 ps

a classical target size. The target size is estimated as πR_0^2 for Xe-Xe collisions and $2\pi R_0^2$ for Xe-Xe_2 collisions, where $R_0=4.4$ Å [15] is the equilibrium separation of the atoms in Xe_2. The potential-well depth of ≈283 K [15] indicates that room-temperature collisions are likely to break up persistent dimers; hence, the corresponding breakup rate $\tau_p^{-1}=k_{\rm Xe}[{\rm Xe}]$ can be estimated by assuming that the breakup coefficient $k_{\rm Xe}$ for persistent dimers by Xe atoms is equal to $\langle\sigma v\rangle_{\rm Xe_2}$. At 295 K and [Xe]=1 amagat we obtain $\tau_p\approx140$ ps, about two orders of magnitude longer than the transient-dimer lifetime τ_t. It is this much longer lifetime that causes persistent dimers (despite their low fractional abundance) to play a dominant role in ^{129}Xe spin relaxation at low densities.

B. Previous studies of ^{129}Xe intrinsic relaxation in the gas phase

More than 40 years ago, Hunt and Carr demonstrated that T_1^{-1} for ^{129}Xe is linearly proportional to the xenon density [Xe] for densities above ≈50 amagat [16]. The dominant source of this intrinsic relaxation is fluctuations in the spin-rotation (SR) interaction, with the Hamiltonian

$$\mathcal{H}_{\rm sr}=c_K(R)\mathbf{K}\cdot\mathbf{N}, \tag{3}$$

where $\mathbf{K}$ is the ^{129}Xe nuclear spin, $\mathbf{N}$ is the angular momentum of the interacting pair of Xe atoms, and $c_K(R)$ is the coupling energy at the distance R between the pair. The linear density dependence suggests that the fluctuations are caused by transient dimers. In the weak-interaction limit, for which $\langle c_K^2N^2\rangle/\hbar^2\ll1$, the corresponding relaxation rate is [13,17]

$$\Gamma_t^{\rm sr}=\sigma_{\rm sr}(T)v_{\rm rms}[{\rm Xe}], \tag{4}$$

where $v_{\rm rms}=(8k_BT/\pi\mu)^{1/2}$ is the relative rms speed of two interacting Xe atoms with reduced mass μ, and $\sigma_{\rm sr}(T)$ is the thermally averaged binary spin-relaxation cross section, which is a function of temperature T and of $c_K(R)$. This work was of necessity carried out at very high xenon densities (tens of amagats) using thermally generated polarization. Extrapolating the data down to [Xe]=1 amagat yields an intrinsic gas-phase T_1 for ^{129}Xe of ≈52 h. This was widely assumed to be the limiting value for several decades, even as SEOP made it common to work with much lower-density xenon samples.

Several years ago, Moudrakovski *et al.* [17] essentially confirmed the results of Hunt and Carr but also found a dependence of the slope of T_1^{-1} vs [Xe] on the square of the applied magnetic field B_0 for [Xe]>20 amagat and B_0 between 4.7 and 9.4 T. This field dependence indicates an additional contribution to the intrinsic relaxation from fluctuations of the chemical shift anisotropy (CSA) interaction. The corresponding Hamiltonian may be written [18]

$$\mathcal{H}_{\rm csa}=c_K(R)\mu_{\rm B}\mathbf{K}\cdot\boldsymbol{\Theta}\cdot\mathbf{B_0}, \tag{5}$$

where $\boldsymbol{\Theta}$ is the inertial tensor of an interacting pair, $\mu_{\rm B}$ is the Bohr magneton, and $c_K(R)$ is the same for both SR and CSA interactions. At such large values of [Xe], the fluctuations were again reasonably presumed to be due to transient dimers. The total intrinsic relaxation rate due to transient dimers is then

$$\Gamma_t=\Gamma_t^{\rm sr}+\Gamma_t^{\rm csa}, \tag{6}$$

where $\Gamma_t^{\rm csa}$ can be written in a form analogous to Eq. (4) with the appropriate cross section $\sigma_{\rm csa}(T)$ depending on B_0^2. The cross sections (and the relaxation rates $\Gamma_t^{\rm csa}$ and $\Gamma_t^{\rm sr}$) become comparable for $B_0=12.5$ T.

Implicit in all of the work involving transient dimers is the assumption of the fast-fluctuation limit. A more complete formulation of the cross sections $\sigma_{\rm sr}(T)$ and $\sigma_{\rm csa}(T)$ would have both multiplied by a factor $1/(1+\Omega^2\tau_c^2)$, where Ω is the Larmor frequency of the nucleus in the applied magnetic field B_0 [19]. (For ^{129}Xe, the Larmor frequency $\Omega=2\pi\times11.78$ MHz/T.) The correlation time τ_c is on the order of the average duration of a binary collision τ_t, or a few picoseconds. The fast-fluctuation limit corresponds to $\Omega^2\tau_t^2\ll1$, which clearly holds for any reasonable B_0. As expected in

this limit, no dependence on applied field was observed up to 2.5 T in the earlier work of Hunt and Carr [16], and the field dependence observed by Moudrakovski *et al.* [17] was due solely to the B_0^2 dependence of the CSA interaction strength.

A key development in understanding intrinsic gas-phase ^{129}Xe relaxation came with the work of Chann *et al.* [13], who presented strong evidence that for lower gas densities typical of SEOP, the fluctuations in the SR interaction are predominantly mediated by the formation and breakup of persistent Xe dimers. Although the fraction of such molecules is small, their lifetime is about two orders of magnitude longer than the transient-dimer lifetime. In the double limit of weak interactions and fast fluctuations, the probability of a spin transition would thus be four orders of magnitude greater for persistent dimers. The further implications of this work are profound: in the low-field limit, the intrinsic ^{129}Xe T_1 at low densities is independent of total gas density and depends instead only on gas composition, i.e., the relative concentrations of xenon and any other gases in the mixture that can serve as an effective third body for the formation and breakup of persistent dimers. Moreover, a maximum possible low-field T_1 for pure xenon gas at room temperature was deduced from these data to be $\approx$4 h, an order of magnitude smaller than the value extrapolated from the work of Hunt and Carr [16].

C. The present work

The purpose of the present work is to investigate ^{129}Xe relaxation due to persistent dimers at high magnetic fields (8.0 T). All previous work has been carried out in the fast-fluctuation limit, for which the dimer lifetime (whether persistent or transient) is much shorter than the ^{129}Xe Larmor period. As [Xe] is reduced below $\approx$1 amagat, an applied field of 8.0 T decouples the relaxation due to persistent dimers; we show that one obtains in this regime a dependence of the rate on total gas density at fixed gas composition that is consistent with the theory of Chann *et al.* [13], including the factor $1/(1+\Omega^2\tau_c^2)$, confirming that persistent and not transient dimers are primarily responsible for intrinsic ^{129}Xe relaxation at these low gas densities. We are able to extract from our data reasonable estimates of molecular formation and breakup parameters, as well as the SR and CSA interaction strengths. The SR interaction strength, properly parametrized according to Ref. [13], allows us to compute for comparison a maximum possible low-field T_1 for pure xenon gas at room temperature of 5.45$\pm$0.2 h, slightly larger than the result of Chann *et al.* [13]. We further confirm both the role of magnetic decoupling and the presence of the CSA interaction at high field with several T_1 measurements for similar gas compositions and total densities in a lower 1.5 T applied field.

The silicone-coated borosilicate-glass cells used in these studies had very low wall-relaxation rates, which was essential in order to investigate the molecular effects with high precision. In the regime where wall relaxation dominates the contribution from persistent dimers, we have measured longitudinal relaxation times $>$25 h at 8.0 T for ^{129}Xe at room temperature.

II. THEORY

The relaxation rate Γ_p of ^{129}Xe due to persistent xenon dimers may be written [13]

$$\Gamma_p = (2\mathcal{K}[\mathrm{Xe}])(M^{\mathrm{sr}} + M^{\mathrm{csa}})\left(\frac{\tau_p}{1+\Omega^2\tau_p^2}\right), \tag{7}$$

where we have slightly rearranged Eq. 2 of Ref. [13] to form the product of three factors. The first factor is the fraction of Xe atoms bound in molecules in accordance with Eq. (2); the second factor $M^{\mathrm{sr}}+M^{\mathrm{csa}}$ is the sum of the SR and CSA mean-square interaction strengths (second moments) during a molecular lifetime, where $M^{\mathrm{csa}} \propto B_0^2$; and the third factor is the power spectrum of magnetic field fluctuations [19], where τ_p is the correlation time for the fluctuations, assumed to be equal to the molecular lifetime. (Here Γ_p and τ_p correspond, respectively, to Γ_{vdW} and τ_B in Ref. [13].) We note that it is immaterial whether the coherent rotation of the persistent dimers is interrupted by collisions that break up the molecule (with on average a new molecule created elsewhere by detailed balance) or by collisions that simply reorient its angular momentum. The inverse correlation time is actually the sum of the rates for these two types of collisions; we call this total rate τ_p^{-1}, since it is likely that purely reorienting collisions are rare in such weakly bound molecules. For linear molecules, the second moments for SR [20] and CSA [21,22] are given by

$$M^{\mathrm{sr}} = \frac{2\langle c_{\vec{k}}^2 N^2\rangle}{3\hbar^2}, \tag{8}$$

$$M^{\mathrm{csa}} = \frac{2}{15}\frac{\mu_{\mathrm{B}}^2 B_0^2}{\hbar^6}\langle c_{\vec{k}}^2 \Theta_\perp^2\rangle, \tag{9}$$

where $\Theta_\perp = \mu R^2$ is the rotational inertia.

Chann *et al.* [13] conducted their experiments in an applied field B_0=20.4 G ($\Omega = 2\pi\times 24$ kHz), for which the CSA interaction is negligible and which corresponds to the fast-fluctuation (low-field) limit at all reasonable gas densities, thus reducing Eq. (7) to

$$\Gamma_p = \frac{4\mathcal{K}\langle c_{\vec{k}}^2 N^2\rangle}{3\hbar^2}[\mathrm{Xe}]\tau_p. \tag{10}$$

For a pure xenon sample in chemical equilibrium, the formation and breakup rate per molecule is $1/\tau_p = k_{\mathrm{Xe}}[\mathrm{Xe}]$, where Xe atoms serve as the third body to provide kinetic energy, and k_{Xe} is the corresponding molecular breakup coefficient. Since $[\mathrm{Xe}]\tau_p$ is a constant, Γ_p is independent of [Xe] in the low-field limit. However, a second gas, capable of serving as a third body in the formation and breakup of molecules, can change τ_p without affecting the fraction of Xe atoms bound in molecules. Chann *et al.* [13] found (and confirmed experimentally) that Γ_p depends on the relative gas composition but not on the total gas density at fixed composition.

For applied magnetic fields on the order of 10 T ($\Omega = 2\pi\times 118$ MHz) and gas densities on the order of 0.1 amagat or lower, we can no longer ignore the $\Omega^2\tau_p^2$ term in the power spectrum of Eq. (7). For fixed B_0, both the SR and CSA terms stay constant, and one should observe the mag-

netic decoupling of relaxation mediated by persistent dimers as the total gas pressure is lowered for a fixed gas composition. We worked exclusively with nitrogen as a second gas and measured Γ_p as a function of total gas pressure for three distinct relative compositions. (An alternative to our experiment would be to vary the density of the second gas while holding [Xe] fixed, which would lead to a maximum in the relaxation rate for $\Omega\tau_p=1$.) We write the molecular breakup rate as

$$\frac{1}{\tau_p} = k_\alpha[G] = k_{\mathrm{Xe}}[\mathrm{Xe}] + k_{\mathrm{N}}[\mathrm{N}_2], \tag{11}$$

where k_{N} is the Xe_2 molecular breakup coefficient for nitrogen and the total gas density $[G]=[\mathrm{Xe}]+[\mathrm{N}_2]$. The overall breakup coefficient k_α is given by

$$k_\alpha = \alpha k_{\mathrm{Xe}} + (1-\alpha)k_{\mathrm{N}}, \tag{12}$$

where $\alpha=[\mathrm{Xe}]/[G]$ is the fractional concentration of xenon. Under our conditions, where [Xe] is small enough to ignore contributions from transient dimers and gradient relaxation is negligible (see Sec. IV), the observed ^{129}Xe relaxation is $\Gamma = \Gamma_w + \Gamma_p$, where Γ_w is the wall relaxation rate. Using Eqs. (7) and (11), we can write Γ as a function of total gas density $[G]$ for a fixed concentration α

$$\Gamma([G]) = \Gamma_w + 2\mathcal{K}(M^{\mathrm{sr}} + M^{\mathrm{csa}})\left(\frac{\alpha k_\alpha[G]^2}{k_\alpha^2[G]^2 + \Omega^2}\right). \tag{13}$$

III. EXPERIMENTAL PROCEDURE AND RESULTS

In order to examine molecular relaxation using Eq. (13), we require stable wall-relaxation rates, where $\Gamma_w < \Gamma_p$. In our early attempts, stability of Γ_w was a problem. Relaxation measurements were done in the same cell that was used to polarize the Xe gas mixture. These cells are similar to those that have been fabricated and used to polarize ^{3}He in our group [23]: They are 5.0 cm diam spheres connected via a 10 cm length of capillary tubing (0.5 mm diam) to a glass valve and side arm for refilling. A 4 cm length of 6 mm glass tubing (the stem) extends from the sphere opposite the capillary entrance. These cells were coated with dichlorodimethylsilane [24] to inhibit wall relaxation and contained a macroscopic amount of Rb metal (tens of milligrams) for optical pumping. Repeated measurements of the room-temperature wall relaxation rate in these cells at 8.0 T showed fluctuations of a factor of two or more. The changes were observed to occur each time after a cell was pumped and polarized at 90 °C. After a cell was polarized several times, Γ_w typically increased (though not necessarily monotonically) to a level comparable to Γ_p or even larger. We infer that at optical pumping temperatures Rb reacted with the coating in a way that ultimately degraded the cell wall lifetime.

Thereafter, we switched to using two distinct types of cells: "pumping" cells and "measurement" cells. Eight different pumping cells (as described above) were used exclusively to generate hyperpolarized ^{129}Xe. Periodically, we found it possible to rejuvenate cells with poor wall rates by removing the Rb, recoating the walls, and distilling in fresh Rb. Xenon gas was transferred from pumping cells to one of two measurement cells (designated 105B and 113B). Measurement cells have a similar geometry to pumping cells and are also coated, but the spherical chamber has a larger 6.7 cm diam. The smaller surface-to-volume ratio in these cells serves to further decrease the wall-relaxation rate. Measurement cells contained no Rb and were never heated above room temperature; they exhibited long and robust wall-relaxation times (>20 h).

Our high-vacuum gas-handling system was used to measure all cell volumes, as well as the ballast volumes used in gas transfer. The same system was also used to fill pumping cells with a precise amount of Xe and N_2, according to the chosen value of the Xe concentration α. A known quantity of Xe atoms was first condensed into the stem of the cell, which was held at 77 K by immersing it in liquid nitrogen. Only the stem was immersed, the rest of the cell remained near room temperature (aided by a small styrofoam heat shield). While the Xe remained frozen, N_2 gas was admitted into the cell at the desired final partial pressure. After filling, the cell was allowed to return completely to room temperature and a final pressure was measured with a separate solid-state gauge (GE Novasensor, Model NPC-410-015A-3L). This final pressure was generally 1–2% higher than targeted; the discrepancy was interpreted as an excess of N_2 because the cell was still somewhat colder than room temperature during filling due to its proximity to the LN_2. This had the effect of slightly lowering the value of α compared to the target value and introducing a small variation. We quote average values for α with an error range reflecting this variation.

Once filled, the gas in a pumping cell was polarized by SEOP with a frequency-narrowed [25] 20 W diode-laser array. The cells were placed in an oven and heated to 90 °C. The oven was located in a 1.5 T superconducting magnet with a 30 cm diam horizontal bore. (The cell capillary protruded laterally outside of the oven so that the valve remained cool.) We found that the 1.5 T field generally decreased the Γ_w of the pumping cell, thus increasing final polarization, as compared to the 30 G Helmholtz arrangement that we initially employed.

Once the Xe gas in a pumping cell was polarized, a known amount of gas was transferred from the pumping cell to a measurement cell, making use of a manifold and, in some cases, ballast volumes in order to achieve a desired total gas density $[G]$. A vacuum pump was used to clear dead spaces and avoid contact with atmospheric oxygen. The gas transfer was performed in the fringe field (≈60 G) of the 8.0 T vertical bore superconducting magnet; the measurement cell was then quickly placed into the NMR probe and the entire assembly secured in the magnet. The probe coil consisted of two elongated loops of wire (a few turns each) positioned on opposite sides of the stem. The coil was tuned to the ^{129}Xe Larmor frequency of 94.1 MHz. The NMR spectrometer incorporates a Tecmag Aries pulse programmer and digitizer with a homebuilt RF section. The longitudinal relaxation rate Γ was measured by the periodic acquisition of the free-induction decay (FID) following the excitation pulse. Since only spins in the relatively small volume of the stem were excited, we were able to use large flip angles while destroying a negligible amount of the total spin mag-

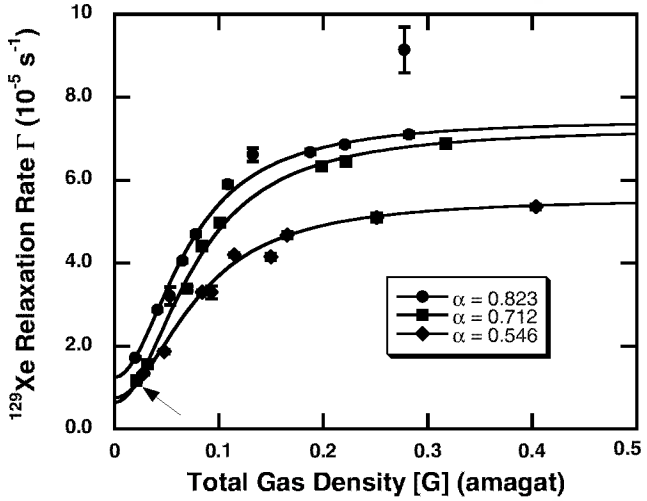

FIG. 1. Plot of ^{129}Xe relaxation rate vs. total gas density at 8.0 T for three values of the concentration $\alpha=[\mathrm{Xe}]/[G]$; the second gas is nitrogen in all cases. The fits are to the theory of Chann *et al.* [13] as parametrized in Eq. (13) and including the CSA interaction. For each value of α, the wall-relaxation rate Γ_w, molecular breakup coefficient k_α, and the product $2\mathcal{K}(M^{\mathrm{sr}}+M^{\mathrm{csa}})$ are extracted from the fits (see Table II). The asymptotes at larger $[G]$ correspond to the density-independent rates observed in Ref. [13], where $k_\alpha^2[\mathrm{G}]^2 \gg \Omega^2$. Relaxation due to persistent dimers is suppressed at low densities, where $k_\alpha[G]=\Omega$ for $[G]$ between about 0.05 and 0.1 amagats. The data point indicated by an arrow corresponds to a measured T_1 of 25 h.

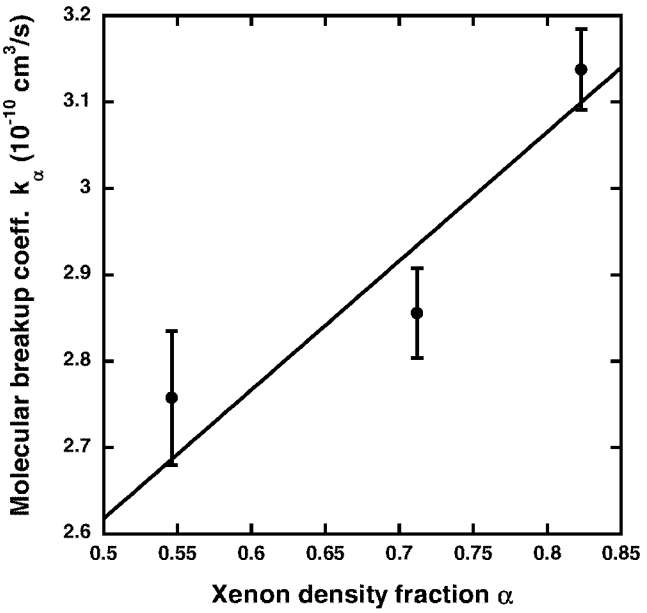

FIG. 2. Plot of molecular breakup coefficient k_α vs fractional xenon density α. The fit is to Eq. (12) and yields molecular breakup coefficients k_{Xe} and k_{N} for xenon and nitrogen, respectively.

netization over the course of the measurement. Either the initial height of each FID or the area of each Fourier-transform peak was plotted vs time of acquisition. The plot was fit to an exponential decay to yield Γ. With the gas depolarized, the solid-state pressure gauge was used again to make a precise measurement of $[G]$. The process of filling and polarizing a pumping cell, transferring gas to a measurement cell, measuring Γ, and measuring $[G]$ was repeated for a range of values of $[G]$ from about 0.02 to 0.4 amagat, to yield Γ vs $[G]$ for each value of α.

Plots of measured relaxation rate Γ at 8.0 T vs total gas pressure $[G]$ are shown in Fig. 1 for three different values of the Xe concentration α. In each case, the data are fit to Eq. (13) with Γ_w, k_α, and $2\mathcal{K}(M^{\mathrm{sr}}+M^{\mathrm{csa}})$ as free parameters. The results are summarized in Table II. Figure 2 is a plot of k_α vs α. The data are fit to Eq. (12), yielding for the molecular breakup coefficients

$$k_{\mathrm{Xe}} = (3.4 \pm 0.1) \times 10^{-10}\ \mathrm{cm}^3/\mathrm{s}, \tag{14}$$

$$k_{\mathrm{N}} = (1.9 \pm 0.2) \times 10^{-10}\ \mathrm{cm}^3/\mathrm{s}. \tag{15}$$

The values of Γ_w extracted from these fits are very small, corresponding to wall-relaxation times of 20–40 h, thus allowing us to observe the dramatic effect of magnetic suppression of the molecular relaxation. The data point for $\alpha=0.712$ and total gas pressure $[G]=0.0215$ amagat (marked in Fig. 1 by an arrow) corresponds to a measured relaxation time of 25 h. The wall relaxation time inferred from the theory exceeds 40 h.

In a separate set of measurements, relaxation data were acquired in the measurement cell 113B for a fixed value of the xenon concentration $\alpha=0.712$ in applied fields of both 8.0 and 1.5 T at several additional values of the total gas density $[G]$. The 1.5 T data were acquired in the same way with a similar NMR spectrometer operating at $\Omega=2\pi \times 17.6$ MHz. The magnet used was the same horizontal bore imaging magnet used to perform SEOP on the pumping cells. The cell was placed on top of a tuned surface coil inside of an aluminum box for shielding. For each value of $[G]$, the relaxation data were acquired consecutively at 1.5 T and then 8.0 T with the same gas, except for the lowest density $[G]=4.9\times10^{-3}$ amagat, for which only data at 1.5 T could be acquired. The results are shown in Fig. 3. The theoretical

TABLE II. Free parameters extracted from the fits of the data in Fig. 1 to Eq. (13) for three values of the Xe concentration α. Errors are given in parentheses for the least significant figure(s). The near constancy of $2\mathcal{K}(M^{\mathrm{sr}}+M^{\mathrm{csa}})$ is evidence for the validity of the persistent-dimer theory of Chann *et al.* [13].

Measurement cell	α	$2\mathcal{K}(M^{\mathrm{sr}}+M^{\mathrm{csa}})$ (10^{-14} cm^3/s^2)	k_α (10^{-10} cm^3/s)	Γ_w (10^{-5} s^{-1})
113B	0.546(4)	2.43(23)	2.76(8)	0.76(5)
113B	0.712(13)	2.66(15)	2.86(5)	0.64(3)
105B	0.823(8)	2.37(8)	3.14(5)	1.25(3)

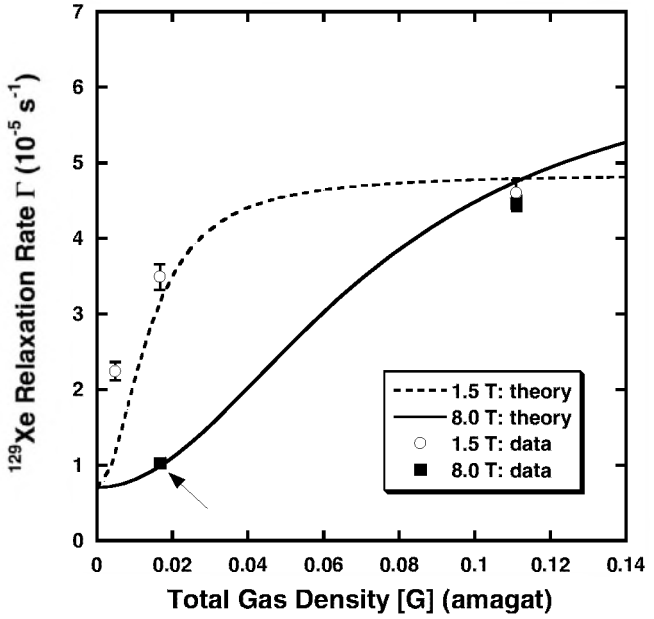

FIG. 3. Plot of ^{129}Xe relaxation rate vs. total gas density at two different applied magnetic fields and a fixed value of the xenon concentration $\alpha=0.712$. All data were acquired using the measurement cell 113B, for which the wall-relaxation rate (intercept of both curves) is taken as 7.0×10^{-6} s^{-1}. For each value of $[G]$, the data were acquired consecutively at 1.5 T and then 8.0 T with the same gas, except for the lowest density point, for which only data at 1.5 T could be acquired. The curves are not fits to the data but rather are predictions derived entirely from the separate and independent data taken and displayed in Fig. 1 and Table II. High-field suppression of the relaxation rate due to persistent dimers is stronger at 8.0 T for low densities, but the larger contribution to relaxation from the CSA interaction at 8.0 T eventually causes the curves to cross near $[G]=0.1$ amagat, where the 1.5 T curve is already well into the limit $\Omega^2\tau_p^2\ll1$. The data point indicated by an arrow corresponds to a measured T_1 of 27.0±1.3 h, the longest gas-phase T_1 ever reported for ^{129}Xe.

curves show the dependence of the rate on $[G]$ for both $B_0=1.5$ T and $B_0=8.0$ T derived exclusively from the analysis of the separate 8.0 T data presented in Fig. 1; the method for arriving at these curves is discussed below.

IV. DISCUSSION

The present work provides strong confirmation of the theory presented by Chann *et al.* [13] for relaxation of gas-phase ^{129}Xe at low densities, particularly through the demonstration of the critical role played by persistent xenon dimers in setting an intrinsic lower bound to the relaxation rate and of high-field suppression of the molecular mechanism, as shown in Fig. 1. The role of transient dimers in our experiments was negligible: our largest xenon density was $[\mathrm{Xe}]\approx0.25$ amagat, for which the contribution to relaxation from transient dimers for $B_0=8.0$ T is $\Gamma_t\approx1.7\times10^{-6}$ s^{-1} [17], four to eight times smaller than the wall-relaxation rates extracted from our fits. The product of the chemical equilibrium coefficient $\mathcal{K}$ and the total second moment $M^{\mathrm{sr}}+M^{\mathrm{csa}}$ (third column of Table II) is dependent strictly on the physics of persistent-dimer formation and of the spin-relaxation interactions, respectively. They cannot be separated experimentally, but the fact that the product remains nearly constant for the three values of Xe concentration α is further evidence for the validity of the persistent-dimer theory. In further analysis below, we will make use of the weighted average

$$2\mathcal{K}(M^{\mathrm{sr}}+M^{\mathrm{csa}})=(2.44\pm0.03)\times10^{-14}\ \mathrm{cm}^3/\mathrm{s}^2. \quad (16)$$

The 1.5 T vs 8.0 T data in Fig. 3 appear to demonstrate the correct dependence of Γ_p on B_0, accounting for the different (and somewhat competing) degrees of both high-field suppression and contribution from the CSA interaction. If we make the reasonable assumption that the ratio $M^{\mathrm{sr}}/M^{\mathrm{csa}}$ is the same for persistent as for transient dimers (still in the weak-interaction limit in all cases), then we can use Ref. [17] to calculate the fraction f of the total interaction strength that is due to SR to be

$$f=\frac{M^{\mathrm{sr}}}{M^{\mathrm{sr}}+M^{\mathrm{csa}}}=(71.0\pm2.7)\ \%\ \text{ at 8.0 T}, \quad (17)$$

whereas $f\approx1$ at $B_0=1.5$ T. The theoretical curves in Fig. 3 have the form of Eq. (13). The intercept for both curves corresponds to $\Gamma_w=7.0\times10^{-6}$ s^{-1}, which is the average of the two extracted values for Γ_w from the two fits in Fig. 1 involving the same measurement cell 113B (see Table II). We used Eqs. (14) and (15) to calculate k_α for $\alpha=0.712$ and the weighted average in Eq. (16), where in the case of $B_0=1.5$ T, $2\mathcal{K}(M^{\mathrm{sr}}+M^{\mathrm{csa}})$ was multiplied by $f(8.0\ \mathrm{T})/f(1.5\ \mathrm{T})\approx f(8.0\ \mathrm{T})$ to account for the much weaker CSA interaction at the lower field. The larger magnetic-field suppression combined with the presence of the CSA interaction for $B_0=8.0$ T causes the curves to cross near $[G]=0.1$ amagat. Near this crossing point, we measured almost identical T_1 values for the two applied fields of about 6 h. Compared to this value, at the lower density $[G]=0.017$ amagat T_1 increases by about 25% at 1.5 T but by more than a factor of four at 8.0 T, due to the stronger magnetic suppression. The latter data point (marked with an arrow in Fig. 3) corresponds to a measured T_1 of 27.0±1.3 h, which is to our knowledge the longest gas-phase relaxation time ever reported for ^{129}Xe.

We have assumed in Fig. 3 that the wall relaxation rate Γ_w is independent of B_0, at least for the two values of B_0 we investigated. The assumption is physically plausible because interactions due to wall collisions should be in the fast-fluctuation limit for all reasonable values of B_0, although the possibility of xenon dissolving into the surface coating [24] potentially complicates this picture. The assumption is also supported by how well the data fall on the curves, which we emphasize are not fits to these data but were derived exclusively from the independent 8.0 T data shown in Fig. 1 and Table II. Finally, even allowing for some field dependence to Γ_w, it is clear from the very low pressure 1.5 T data point ($[G]=4.9\times10^{-3}$ amagat), where T_1 is over 12 h, that the difference in relaxation rates for $[G]=0.017$ amagat could not be explained by a difference in Γ_w alone.

Using Eqs. (16) and (17), and the value $\mathcal{K}=230$ Å^3 calculated in Ref. [13], we can make an estimate of the SR interaction strength $M^{\mathrm{sr}}=3.77\times10^7$ s^{-2}. Using Eq. (8), we obtain

$$\sqrt{\langle c_K^2 N^2\rangle} = h \times 1200 \text{ Hz}. \tag{18}$$

This value falls between two estimates made by Chann *et al.* [13], one of 820 Hz based on their measurement of the low-field pure-xenon relaxation rate [see Eq. (22) below] and the relationship between the SR coupling and the Xe-Xe chemical shift [26–28], and the other of 1400 Hz based on the measured spin-relaxation rate due to transient dimers in the applied-field regime where the CSA interaction is negligible [16,17]. These estimates and our result imply a value for $c_K(R_0)/h$ (where R_0 is the equilibrium separation) of between 20 and 40 Hz, consistent with *ab initio* results of ≈30 Hz [15]. Using a similar argument and the fraction $1-f$ of the total interaction strength that is due to CSA, along with Eq. (9), we estimate

$$\sqrt{\langle c_K^2 R^4\rangle} = h \times 240 \text{ Hz Å}^2, \tag{19}$$

which is consistent with $c_K(R_0)/h \approx 10$ Hz. We note that the CSA interaction is related to the anisotropic chemical shift $\Delta\sigma$ of the xenon dimer by [22]

$$\Delta\sigma = \sigma_\parallel - \sigma_\perp = -\frac{\mu_B \Theta_\perp c_K(R)}{\gamma\hbar^3}, \tag{20}$$

where γ is the ^{129}Xe gyromagnetic ratio. However, the extremely short correlation times in the gas phase do not readily permit direct NMR measurements of $\sigma_\parallel$ and $\sigma_\perp$.

Our values for k_{Xe} and k_{N} are quite reasonable compared to the estimates based on kinetic theory. In fact, our estimated velocity-averaged cross section for collisions between xenon dimers and xenon atoms is within 20% of the value of k_{Xe} in Eq. (14) (see Table I), supporting our assumption that most collisions result in the breakup of the weakly bound persistent dimers. We find nitrogen as a third body to be only about half as efficient as Xe, somewhat in disagreement with the results of Chann *et al.* [13], who measured the ratio $k_{\mathrm{N}}/k_{\mathrm{Xe}}$ to be close to unity and deduced a breakup rate $k_{\mathrm{Xe}}=1.2\times10^{-10}$ cm^3/s, where the latter number is based on the calculated 820 Hz estimate for $\sqrt{\langle c_K^2 N^2\rangle}/h$ discussed above.

We can make a further comparison to the results of Chann *et al.* [13] by considering the low-field limit ($\Omega^2 \ll k_\alpha^2[G]^2$) of Eq. (13). Ignoring the CSA interaction and using Eq. (8), we obtain

$$\Gamma([G]) = \Gamma_w + \frac{4\mathcal{K}\langle c_K^2 N^2\rangle \alpha}{3\hbar^2 k_\alpha}. \tag{21}$$

In the limit where $\alpha=1$ and $k_\alpha=k_{\mathrm{Xe}}$, we obtain what is called $\Gamma_{\mathrm{vdW}}^{\mathrm{Xe}}$ in Ref. [13], the low-field pure-xenon relaxation rate due to persistent dimers

$$\Gamma_{\mathrm{vdW}}^{\mathrm{Xe}} k_{\mathrm{Xe}} = \frac{4\mathcal{K}\langle c_K^2 N^2\rangle}{3\hbar^2}. \tag{22}$$

We can write an equivalent expression that is appropriate for our data using Eq. (17) to account for our 8.0 T applied field

$$\Gamma_{\mathrm{vdW}}^{\mathrm{Xe}} k_{\mathrm{Xe}} = 2\mathcal{K}(M^{\mathrm{sr}} + M^{\mathrm{csa}}) f(8.0 \text{ T}). \tag{23}$$

Using our values for k_{Xe} and $f(8.0\text{ T})$ in Eqs. (14) and (17), and the weighted average of $2\mathcal{K}(M^{\mathrm{sr}}+M^{\mathrm{csa}})$ in Eq. (16), we find

$$\Gamma_{\mathrm{vdW}}^{\mathrm{Xe}} = (5.1\pm0.2)\times10^{-5} \text{ s}^{-1}, \tag{24}$$

which corresponds to a limiting low-field relaxation time for pure xenon of 5.45±0.2 h, slightly larger than Chann *et al.*'s value [13] of 4.1±0.1 h.

Relaxation due to diffusion of ^{129}Xe through magnetic-field gradients in Eq. (1) should be negligible in our experiments. We confirmed this by displacing the entire cell and probe vertically by as much as 4 cm and recording the change in NMR frequency. We estimated a gradient of ≈3G/cm in the 8.0 T magnet. (The relative gradients were even smaller in the 1.5 T magnet.) In the regime where the diffusion time across the cell is much longer than the Larmor period [10], gradient relaxation is given by

$$\Gamma_g = D\frac{|\nabla B_\perp|^2}{B_0^2}, \tag{25}$$

where $\nabla B_\perp$ is the transverse magnetic field gradient and D is the Xe diffusion coefficient. Even in the fastest-diffusion case of a cell containing 0.01 amagat of pure xenon, Eq. (25) predicts $T_1 > 10^8$ s from this mechanism alone.

It is possible that there are contributions to our measured relaxation rates from persistent Xe-N_2 dimers [29], producing another molecular term in Eq. (13) with a different chemical-equilibrium coefficient, interaction strength, and molecular lifetime. These molecules are somewhat more weakly bound, having well depth ϵ/k_B between 200 and 250 K [29]. In addition to the quality of our fits to a model involving only Xe_2 dimers, we rely on the results and conclusions of Chann *et al.* [13], where the asymptotic relaxation rate at high second-gas densities approached a common value (the wall-relaxation rate for the one cell employed) for Ar, N_2, and He gases. This result is relevant because the well depth for Xe-He is exceedingly small at ≈30 K; the asymptotic rates should have been different for the different second gases had the corresponding dimers played a significant role in relaxation. They were thus lead to conclude that Xe-N_2 dimers are not contributing significantly to the measured relaxation rates, and there is no reason to expect this to change at higher applied fields.

It is likely that in some earlier work [17,30] at lower xenon densities, Γ_w was inadvertently overestimated due to a significant contribution from the molecular mechanism. For example, Breeze *et al.* [30] measured $\Gamma^{-1}\approx3$ h in cells containing ≈1 amagat of xenon and a relatively small amount of nitrogen, attributing virtually all of this relaxation to wall interactions. For this density and their applied field of 4.7 T, we would predict $\Gamma_p^{-1}=4.4$ h; the actual wall relaxation time $(\Gamma-\Gamma_p)^{-1}$ would then be almost 10 h.

Variations in the applied field B_0 and/or the total gas density $[G]$ at fixed xenon concentration α thus lead to changes in two distinct aspects of the relaxation due to persistent dimers: the rate of fluctuations compared to Ω, and the rela-

tive strengths of the CSA and SR interactions. In the regime where B_0 is below several tesla, the fast-fluctuation limit $\Omega^2\tau_p^2 \ll 1$ (low field and high density, as in Ref. [13]) leads to an intrinsic relaxation that is independent of both $[G]$ and B_0. In the opposite limit of slow fluctuations (high field but still SR-dominated, and low density) the intrinsic relaxation is proportional both to $[G]^2$ and to $1/B_0^2$. In the regime where $B_0 > 10$ T, the CSA interaction begins to dominate, and relaxation in the fast-fluctuation limit, while still density independent, is now proportional to B_0^2. In the limit of slow fluctuations, the relaxation still depends on $[G]^2$ but becomes independent of B_0 as the effects of the CSA interaction and slow fluctuations cancel each other. We note that (according to our value for k_{Xe}) $\Omega\tau_p = 1$ for $B_0/[G] \approx 120$ T/amagat for pure xenon, so that the fast-fluctuation limit is readily attained for densities ≈ 1 amagat, even for very large laboratory magnetic fields, and the fast-fluctuation limit *always* holds for B_0 at or below ≈ 0.1 T, where the gas densities otherwise start to become too low to be detectable by NMR (even when hyperpolarized). Our data straddle both the transition from near-zero to moderate CSA interaction strength and the transition from the slow- to the fast-fluctuation limit. Finally, for completeness we note that the contribution to relaxation from transient dimers (always in the fast-fluctuation limit and linearly dependent on [Xe]) becomes equal to that from persistent dimers for $[\mathrm{Xe}] \approx 10$ amagats, with a B_0^2 dependence coming in at the largest applied fields.

The extraordinarily long T_1 values for gas-phase ^{129}Xe measured here have potential implications for accumulating and storing large quantities of hyperpolarized xenon. We have fabricated cells with sufficiently low wall-relaxation rates ($< 1/20\ \mathrm{h}^{-1}$) that the maximum $T_1 \approx 5$ h due to the molecular mechanism for pure xenon samples can be realized in practice. Many designs for accumulation are based on storing hyperpolarized Xe frozen at 77 K [31,32], where T_1 of the solid is only 2.5 h [33], and one must adequately address potential polarization losses due to the freeze-thaw cycle. The use of an 8.0 T magnet in a practical device is clearly cumbersome, but there is strong evidence that the wall-relaxation rates in our cells do not increase by much for B_0 as low as 1.5 T. Much longer T_1 values are possible, although these are currently realized only for gas compositions that are lean in Xe and/or have total gas densities ≤ 0.1 amagat. However, given that the Xe_2 potential-well depth ϵ/k_B is so close to room temperature, increasing the temperature by even a few tens of degrees Celsius may significantly decrease the limiting relaxation rates due to persistent dimers and greatly improve prospects for a room-temperature accumulator at xenon densities approaching 1 amagat. Additional experiments to look for the B_0^2 dependence at relatively high applied magnetic fields would better sort out the contributions from the spin-rotation and chemical-shift-anisotropy interactions, as well as any variable wall-relaxation rate, in order to find the optimal field in which to operate a practical device.

ACKNOWLEDGMENTS

We are grateful to D. C. Ailion for the use of equipment and helpful discussions, to M. S. Conradi and C. J. Jameson for helpful comments and discussions, and to K. Teaford for assistance with cell fabrication. This work was supported by the National Science Foundation Grant No. PHY-0134980.

[1] T. G. Walker and W. Happer, Rev. Mod. Phys. **69**, 629 (1997).
[2] S. Appelt, A. B. Baranga, C. J. Erickson, M. V. Romalis, A. R. Young, and W. Happer, Phys. Rev. A **58**, 1412 (1998).
[3] E. Babcock, B. Chann, T. G. Walker, W. C. Chen, and T. R. Gentile, Phys. Rev. Lett. **96**, 083003 (2006).
[4] M. S. Conradi, B. T. Saam, D. A. Yablonskiy, and J. C. Woods, Prog. Nucl. Magn. Reson. Spectrosc. **48**, 63 (2006).
[5] H. E. Möller, X. J. Chen, B. Saam, K. D. Hagspiel, G. A. Johnson, T. A. Altes, E. E. de Lange, and H.-U. Kauczor, Magn. Reson. Med. **47**, 1029 (2002).
[6] K. Ruppert, J. F. Mata, J. R. Brookeman, K. D. Hagspiel, and J. P. Mugler III, Magn. Reson. Med. **51**, 676 (2004).
[7] M. M. Spence, E. J. Ruiz, S. M. Rubin, T. J. Lowery, N. Winssinger, P. G. Schultz, D. E. Wemmer, and A. Pines, J. Am. Chem. Soc. **126**, 15287 (2004).
[8] H. J. Jänsch, P. Gerhard, and M. Koch, Proc. Natl. Acad. Sci. U.S.A. **101**, 13715 (2004).
[9] N. R. Newbury, A. S. Barton, G. D. Cates, W. Happer, and H. Middleton, Phys. Rev. A **48**, 4411 (1993).
[10] G. D. Cates, S. R. Schaefer, and W. Happer, Phys. Rev. A **37**, 2877 (1988).
[11] L. D. Shearer and G. K. Walters, Phys. Rev. **139**, A1398 (1965).
[12] N. Bernardes and H. Primakoff, J. Chem. Phys. **30**, 691 (1959).
[13] B. Chann, I. A. Nelson, L. W. Anderson, B. Driehuys, and T. G. Walker, Phys. Rev. Lett. **88**, 113201 (2002).
[14] F. Reif, *Fundamentals of Statistical and Thermal Physics* (McGraw-Hill, New York, 1965).
[15] M. Hanni, P. Lantto, N. Runeberg, J. Jokisaari, and J. Vaara, J. Chem. Phys. **121**, 5908 (2004).
[16] E. R. Hunt and H. Y. Carr, Phys. Rev. **130**, 2302 (1963).
[17] I. L. Moudrakovski, S. R. Breeze, B. Simard, C. I. Ratcliffe, J. A. Ripmeester, T. Seideman, and J. S. Tse, J. Chem. Phys. **114**, 2173 (2001).
[18] N. N. Kuzma, D. Babich, and W. Happer, Phys. Rev. B **65**, 134301 (2002).
[19] N. Bloembergen, E. M. Purcell, and R. V. Pound, Phys. Rev. **73**, 679–712 (1948).
[20] P. S. Hubbard, Phys. Rev. **131**, 1155 (1963).
[21] H. M. McConnell and C. H. Holm, J. Chem. Phys. **25**, 1289 (1956).
[22] H. W. Spiess, D. Schweizer, U. Haeberlen, and K. H. Hausser, J. Magn. Reson. (1969-1992) **5**, 101 (1971).
[23] R. E. Jacob, S. W. Morgan, and B. Saam, J. Appl. Phys. **92**, 1588 (2002).

[24] B. Driehuys, G. D. Cates, and W. Happer, Phys. Rev. Lett. **74**, 4943 (1995).
[25] B. Chann, I. Nelson, and T. G. Walker, Opt. Lett. **25**, 1352 (2000).
[26] N. F. Ramsey, Phys. Rev. **78**, 699 (1950).
[27] H. C. Torrey, Phys. Rev. **130**, 2306 (1963).
[28] C. J. Jameson, A. K. Jameson, and S. M. Cohen, J. Chem. Phys. **62**, 4224 (1975).
[29] A. C. de Dios and C. J. Jameson, J. Chem. Phys. **107**, 4253 (1997).
[30] S. R. Breeze, S. Lang, I. Moudrakovski, C. I. Ratcliffe, J. A. Ripmeester, G. Santyr, B. Simard, and I. Zuger, J. Appl. Phys. **87**, 8013 (2000).
[31] B. Driehuys, G. D. Cates, E. Miron, K. Sauer, D. K. Walter, and W. Happer, Appl. Phys. Lett. **69**, 1668 (1996).
[32] I. C. Ruset, S. Ketel, and F. W. Hersman, Phys. Rev. Lett. **96**, 053002 (2006).
[33] M. Gatzke, G. D. Cates, B. Driehuys, D. Fox, W. Happer, and B. Saam, Phys. Rev. Lett. **70**, 690 (1993).